

Particle simulation of Coulomb collisions: Comparing the methods of Takizuka & Abe and Nanbu

Chiaming Wang^{a,*}, Tungyou Lin^a, Russel Caflisch^a,
Bruce I. Cohen^b, Andris M. Dimits^b

^a *Mathematics Department, University of California at Los Angeles, Los Angeles, CA 90036, USA*

^b *Lawrence Livermore National Laboratory, Livermore, CA 94550, USA*

Received 21 May 2007; received in revised form 6 November 2007; accepted 13 December 2007

Available online 19 January 2008

Abstract

The interactions of charged particles in a plasma are governed by long-range Coulomb collision. We compare two widely used Monte Carlo models for Coulomb collisions. One was developed by Takizuka and Abe in 1977, the other was developed by Nanbu in 1997. We perform deterministic and statistical error analysis with respect to particle number and time step. The two models produce similar stochastic errors, but Nanbu's model gives smaller time step errors. Error comparisons between these two methods are presented.

Published by Elsevier Inc.

1. Introduction

A plasma consists of a large number of charged particles. An appropriate method to describe a plasma state is a statistical approach, *i.e.*, a distribution function provides a complete description of the system. If a plasma is highly collisional, its distribution function will be rapidly driven to thermodynamical equilibrium, and the plasma kinetics can be approximated by a fluid description. On the other hand, if a plasma is collisionless, the plasma is not necessarily in equilibrium, and each particle interacts with the rest of the plasma through the collective effects of long-range electromagnetic fields. In the intermediate regime between the two cases, collisional effects have to be included specifically to provide an adequate description of plasma kinetics. One significant example is the edge plasma (scrape-off layer) in a confinement fusion device. A fluid approximation is not valid since the high energy (superthermal) electrons result in a relatively large ratio of the mean free path to the system's characteristic length. A kinetic approach is essential for satisfactory physical modeling and numerical simulations for such plasmas [1].

* Corresponding author.

E-mail address: cmwang@ucla.edu (C. Wang).

One feature which distinguishes a plasma from a fluid is that its particles are charged and have long-range Coulomb interactions. A particle in a plasma has distant encounters with many other particles simultaneously, and each encounter produces a small collisional effect on the particle. The scattering of particles due to multiple small collisions is dominant and is more important than the single large-angle scattering. For this reason, the Coulomb scattering angle can be treated as the cumulative deflection of a series of small-angle binary collisions [2].

One of the earliest and most influential Monte Carlo binary collision models was proposed by Takizuka & Abe in 1977 [3]. In their method, the domain is divided into cells and particles are grouped within each cell. Randomly chosen pairs of particles undergo binary collisions. The resulting scattering angle is sampled through a Gaussian distribution to compute the change in velocities. Their method simulates each small-angle collision and requires a time step much smaller than the overall relaxation time for the entire velocity distribution function.

Nanbu proposed a new Monte Carlo binary collision model in 1997 [4]. His method uses the idea that a Coulomb collision can be described by many continuous small-angle binary collisions [2]. Nanbu's method computes the cumulative scattering angle for many small binary deflections. Successive small angles are grouped into one single collision angle. This suggests that a larger time step may be used in his method.

The two methods proposed by Takizuka & Abe and Nanbu have been widely used in the plasma physics community. Nanbu's method has been considered more efficient than Takizuka & Abe's method because it computes a cumulative Coulomb scattering angle rather than a single Coulomb scattering angle one by one. For this reason, we are interested in performing a convergence analysis to compute the errors and to derive the orders of accuracy for both methods to quantitatively compare their performance and relative efficiencies. We also believe these models have the potential to be used to extend the hybrid method for rarefied gas dynamics [5] to a plasma with Coulomb collisions.

For simplicity, in this article we call the collision model developed by Takizuka and Abe "TA's method" and the model developed by Nanbu "Nanbu's method". To test these two models, we use a test problem that consists of a spatially homogeneous plasma with no electric or magnetic fields, as described in [3,4]. We simulate the relaxation of an anisotropic Maxwellian distribution (*i.e.*, a distribution with anisotropic temperatures) over time due to collisions, using the results to evaluate the accuracy and efficiency of these two methods. We test both electron–electron and electron–ion collision cases and obtain comprehensive convergence results. We find a few similarities of the results computed using the two methods. For the average solutions, both methods have square root of the time step accuracy $O(\sqrt{\Delta t})$. The random errors are independent of time step, and diminish like $O(N^{-\frac{1}{2}})$ when the number of particles N grows. In the conclusion, we evaluate the significance of the results, as well as consider some advantages to Nanbu's method and its possible applications.

The article is organized as follows. First we describe the collision models formulated by Takizuka & Abe, and Nanbu in Section 2. In Section 3, we propose a test case and define the quantities for the convergence analysis. Next, we present the simulation results for Nanbu's method and TA's method, and compare the differences in the results obtained in Section 4. Concluding remarks and a summary are offered in Section 5.

2. General formulation

We first introduce the governing equation for the physical process, and describe TA and Nanbu's Monte Carlo binary collision models. We will emphasize the major distinguishing aspect of the two collision models: computing the scattering angle of two colliding particles. We consider collisions between N particles from two species α and β . For simplicity, we assume that N is even. If α and β are the same, we assume that there are $N/2\alpha$ particles and $N/2\beta$ particles. If α and β are different, then there are $N\alpha$ particles and $N\beta$ particles.

2.1. Governing equation

The time evolution of the particle distribution in a non-equilibrium plasma is described by the Fokker–Planck equation:

$$\frac{\partial f_\alpha}{\partial t} + \mathbf{v} \cdot \nabla_x f_\alpha + \frac{e}{m_\alpha} (E + \mathbf{v} \times B) \cdot \nabla_v f_\alpha = \left(\frac{\delta f_\alpha}{\delta t} \right)_c$$

$$f_\alpha(\mathbf{v}, \mathbf{x}, 0) = f_{\alpha 0}(\mathbf{v}, \mathbf{x})$$

where f_α is the distribution function of the α species, m_α is the mass of the α species, E is the electric field, B is the magnetic field. $\left(\frac{\delta f_\alpha}{\delta t} \right)_c$ is the collision operator and defined as the following:

$$\left(\frac{\delta f_\alpha}{\delta t} \right)_c = - \sum_\beta \frac{\partial}{\partial v_j} \frac{e_\alpha^2 e_\beta^2 \log A}{8\pi\epsilon_0^2 m_\alpha} \int d\mathbf{v}' \left[\frac{\delta_{jk}}{u} - \frac{u_j u_k}{u^3} \right] \left[\frac{f_\alpha}{m_\beta} \frac{\partial f_\beta(v')}{\partial v'_k} - \frac{f_\beta(v')}{m_\alpha} \frac{\partial f_\alpha}{\partial v_k} \right] \tag{1}$$

where $\log A$ is the Coulomb logarithm. The equation for f_β is similar. The collision operator defined in (1) is called the Landau–Fokker–Planck collision operator [6].

TA and Nanbu’s collision models can be considered as numerical approximations to the Fokker–Planck collision operator. We will discuss the two models for a spatially homogeneous plasma in the following two sections.

2.2. Takizuka and Abe’s collision model

The scattering angle in TA’s method is defined in the relative velocity frame. First two particles with velocity v_α and v_β are selected. Let Θ be the scattering angle between two particles in the relative frame. The angle Θ is sampled randomly through a random variable δ related to Θ by the function \tan . Specifically,

$$\delta \equiv \tan(\Theta/2) \tag{2}$$

where δ is a Gaussian random variable which has mean 0 and the following variance

$$\langle \delta^2 \rangle = \left(\frac{e_\alpha^2 e_\beta^2 n_L \log A}{8\pi\epsilon_0^2 m_{\alpha\beta}^2 u^3} \right) \Delta t$$

where e_α and e_β are electric charges for the species α and β , n_L is the smaller density of the particle species α and β , A is the Coulomb logarithm, $u = |v_\alpha - v_\beta|$ is the relative speed, Δt is the time step, and $m_{\alpha\beta}$ is the reduced mass and is defined as follows:

$$m_{\alpha\beta} = \frac{m_\alpha m_\beta}{m_\alpha + m_\beta}.$$

To compute the velocity changes of the particles due to collision, a Gaussian random variable δ is sampled and used to compute $\sin \Theta$ and $\cos \Theta$ through the following formulas derived from (2):

$$\sin \Theta = \frac{2\delta}{(1 + \delta^2)}$$

$$1 - \cos \Theta = 2\delta^2 / (1 + \delta^2).$$

$\sin \Theta$ and $\cos \Theta$ are then used to compute the postcollisional velocities v'_α, v'_β of the two particles [3].

$$v'_\alpha = v_\alpha + \frac{m_{\alpha\beta}}{m_\alpha} \Delta u$$

$$v'_\beta = v_\beta - \frac{m_{\alpha\beta}}{m_\beta} \Delta u$$

and Δu is defined as follows:

$$u = v_\alpha - v_\beta,$$

$$\Delta u_x = (u_x/u_\perp)u_z \sin \Theta \cos \Phi - (u_y/u_\perp)u \sin \Theta \sin \Phi - u_x(1 - \cos \Theta),$$

$$\Delta u_y = (u_y/u_\perp)u_z \sin \Theta \cos \Phi + (u_x/u_\perp)u \sin \Theta \sin \Phi - u_y(1 - \cos \Theta),$$

$$\Delta u_z = -u_\perp \sin \Theta \cos \Phi - u_z(1 - \cos \Theta),$$

and $u_\perp = \sqrt{u_x^2 + u_y^2}$. The azimuthal angle Φ is randomly chosen from the uniform interval $[0, 2\pi]$.

In each time step, TA’s method groups all of the N particles into $N/2$ pairs, each consisting of an alpha particle and a beta particle, and performs a single collision for each pair. The random selection of particle pairs through many time steps approximates the integration of the distribution function over the particles. The method’s cross section represents the Fokker–Planck process. Hence, TA’s method directly simulates the Fokker–Planck collision operator (1).

2.3. Nanbu’s collision model

Coulomb collisions in a plasma can be treated as the simulation of many continuous small-angle binary collisions [2]. Rather than computing every small-angle binary collision as in TA’s method, Nanbu’s method provides a procedure to compute the aggregated scattering angle of many small angle binary collisions for a given pair of velocities v_α and v_β .

Let \mathbf{g}_0 be the initial velocity and $\mathbf{g}_1, \mathbf{g}_2, \dots, \mathbf{g}_N$ be the postcollision velocities after first, second, \dots , and N collisions. Let χ_N be the cumulative scattering angle after N collisions. χ_N is defined as the following

$$\cos \chi_N = \mathbf{g}_0 \cdot \mathbf{g}_N / g^2$$

where $g = |\mathbf{g}_0|$. χ_N can be obtained through the following three steps:

1. At the beginning of the time step, calculate a quantity s

$$s = n_\beta g \pi b_0^2 (\ln A) \Delta t$$

where b_0 is the impact parameter, n_β is the density of field particles, A is the Coulomb logarithm and Δt is the time step.

2. Use s to determine a constant A from the following equation:

$$\coth A - A^{-1} = e^{-s}.$$

The constant A will be used to define the probability density of χ_N .

3. Sample the cumulative scattering angle χ_N with the following probability density function $F(\chi_N)$:

$$F(\chi_N) = \frac{2\pi A}{4\pi \sinh A} e^{A \cos \chi} \sin \chi_N.$$

The velocities after cumulative collisions are

$$\begin{aligned} \mathbf{v}'_\alpha &= \mathbf{v}_\alpha - \frac{m_{z\beta}}{m_\alpha} [\mathbf{g}(1 - \cos \chi) + \mathbf{h} \sin \chi], \\ \mathbf{v}'_\beta &= \mathbf{v}_\beta + \frac{m_{z\beta}}{m_\beta} [\mathbf{g}(1 - \cos \chi) + \mathbf{h} \sin \chi], \end{aligned}$$

where $\mathbf{g} = \mathbf{v}_\alpha - \mathbf{v}_\beta$ and $\mathbf{h} = (h_x, h_y, h_z)$ with

$$\begin{aligned} h_x &= g_\perp \cos \epsilon, \\ h_y &= -(g_y g_x \cos \epsilon + g g_z \sin \epsilon) / g_\perp, \\ h_z &= -(g_z g_x \cos \epsilon - g g_y \sin \epsilon) / g_\perp, \end{aligned}$$

and $g_\perp = \sqrt{g_y^2 + g_z^2}$ and ϵ is a random number uniformly distributed in $[0, 2\pi]$.

Nanbu’s method is motivated by physical considerations associated with Coulomb collisions in the Fokker–Planck limit. In a subsequent work, Bobylev and Nanbu [7] derived a time–explicit formula to approximate the time evolution of plasmas from the Boltzmann equation. Their analysis theoretically verifies that, when $\Delta t \rightarrow 0$, the numerical solutions computed using Nanbu’s method are the solutions of the Fokker–Planck equation. More specifically, the method approximates the collision operator J of the Boltzmann equation by an exponential operator defined by J and then solves an initial-value problem using spherical harmonic

functions to define the time evolution formula. Similar to the idea that is used to derive Fokker–Planck equation from the Boltzmann equation [8], small-angle scattering leads to the formula for computing the evolution of a velocity distribution:

$$f_{\alpha}(\mathbf{v}, t + \Delta t) = \sum_{\beta=1}^n \pi_{\alpha\beta} \int_{R^3 \times S^2} d\mathbf{w} d\mathbf{n} D_{\alpha\beta} \left(\frac{\mathbf{g} \cdot \mathbf{n}}{g}, A \frac{\Delta t}{g^3} \right) f_{\alpha}(\mathbf{v}'_{\alpha}, t) f_{\beta}(\mathbf{v}'_{\beta}, t).$$

The function $D_{\alpha\beta}$ is defined by an infinite sum of Legendre polynomials, see [7] for details. Within an error of $O(\Delta t)$, $D_{\alpha\beta}$ can be further approximated by functions which are simpler and easier to be computed. In particular, D_{\star} can be defined as follows:

$$D_{\star}(\mu, \tau) = \frac{A}{4\pi \sinh A} \exp \mu A.$$

In this case, the distribution of accumulated scattering angle of Nanbu's method is $F(\chi_N) = 2\pi \sin \chi_N D_{\star}(\cos \frac{\chi_N}{2}, \frac{\delta}{2})$, and the method may be considered as a special case of a general framework developed in [7]. We note that both TA and Nanbu's methods integrate the Fokker–Planck equation from t to $t + \Delta t$ with an explicit scheme using only velocity distribution function data evaluated at t ; such an integration scheme is no better than first-order accurate in Δt . Error accumulation in the TA and Nanbu methods is examined in the convergence results in Section 4.

3. Test case and definitions

We perform simulations for the equilibration of a plasma which has a spatially homogeneous distribution function with anisotropic initial temperature for an electron–electron case and for an electron–ion collision case. Due to the statistical nature of the Monte Carlo model, we extract the deterministic errors by computing the mean of multiple statistically independent solutions. The statistical errors are computed using the empirical variance of these solutions. The comparison includes both the deterministic errors and statistical errors when the time steps or number of particles are varied. The error in the numerical solution is evaluated by comparing it to a highly accurate solution, using a very small time step and a large number of particles.

3.1. Test case

Our task is to compare the accuracy of the two collision models. For this reason, we assume spatial homogeneity and that no electric or magnetic fields exist in the system, and no flow. Then the physical governing equation becomes the following:

$$\frac{\partial f_{\alpha}}{\partial t} = \left(\frac{\delta f_{\alpha}}{\delta t} \right)_{\text{c}}$$

$$f_{\alpha}(\mathbf{v}, 0) = f_{\alpha 0}(\mathbf{v}).$$

TA and Nanbu's collision methods are numerical approximations to the analytic model of the Fokker–Planck collision term $\left(\frac{\delta f_{\alpha}}{\delta t} \right)_{\text{c}}$.

We consider the time relaxation of charged particles due to electron and electron collisions or electron and ion collisions. The initial distribution has small anisotropy, *i.e.*, the parallel temperature and the perpendicular temperature are slightly different, as shown in Fig. 1 at $t = 0$. Specifically, we use $T_z = 0.008$ and $T_p = 0.01$ for our simulation. These temperatures are nominal and used to generate the velocities of particles. The actual temperatures could be slightly different from the given temperatures T_z and T_p due to statistical sampling. All the temperatures (*i.e.* temperature difference) shown in the simulation results are actual and are computed using velocity distributions of the particles.

An approximate analytic solution of the test case was derived in [9] using the Fokker–Planck equation in Landau form and assuming small temperature anisotropy. In [9] the initial distribution is assumed to be the following:

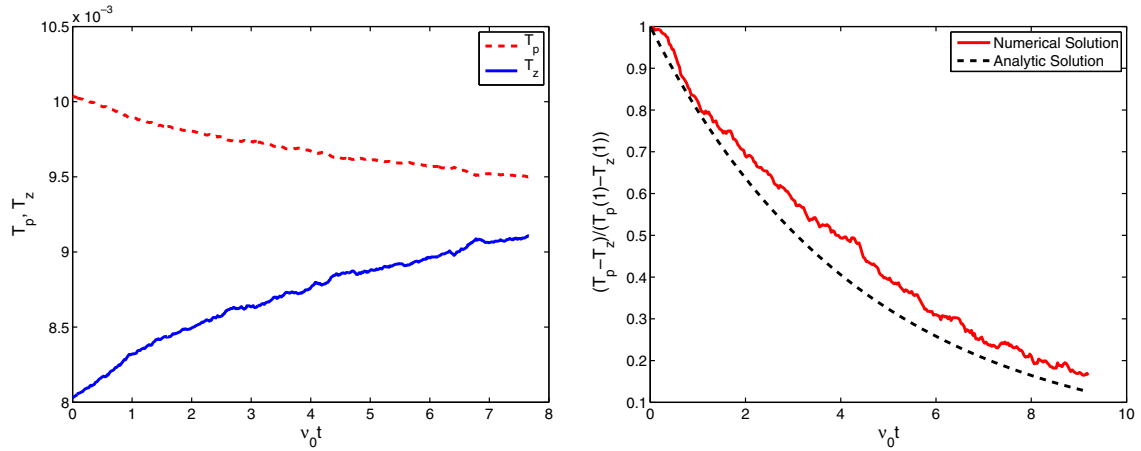


Fig. 1. Time relaxation of anisotropic temperatures due to collisions.

$$f_0(0, \mathbf{v}) = \left(\frac{m}{2\pi}\right)^{3/2} \frac{1}{\sqrt{T_{\parallel}T_{\perp}}} \exp\left(-\frac{mv_{\parallel}^2}{2T_{\parallel}} - \frac{mv_{\perp}^2}{2T_{\perp}}\right).$$

The temperature T of the system is

$$T = \frac{1}{3}T_{\parallel} + \frac{2}{3}T_{\perp}.$$

The conservation of the kinetic energy implies T is constant at all time, hence we have

$$\frac{dT_{\perp}}{dt} = -\frac{1}{2} \frac{dT_{\parallel}}{dt} = \int \frac{df}{dt} \frac{mv_{\parallel}^2}{2} dv.$$

Replacing $\frac{df}{dt}$ by the Fokker–Planck operator, and assuming $|T_{\parallel} - T_{\perp}| < T_{\parallel}$, the following equation was derived:

$$\frac{dT_{\perp}}{dt} = -\frac{1}{2} \cdot \frac{dT_{\parallel}}{dt} = -\frac{T_{\perp} - T_{\parallel}}{\frac{15}{8}\sqrt{2\pi}\tau_0(T)}$$

then

$$\begin{aligned} \frac{d\Delta T}{dt} &= 3 \cdot \frac{dT_{\perp}}{dt} = -\frac{\Delta T}{\tau} \\ \tau &= \frac{5}{8}\sqrt{2\pi}\tau_0(T), \end{aligned}$$

and

$$\tau_0(T) = \frac{\sqrt{m_x}}{\pi\sqrt{2}e_x^4} \frac{T^{3/2}}{\ln \Lambda n_x}.$$

Then we have

$$\Delta T(t) = \Delta T e^{-t/\tau}.$$

3.2. Simulations

We perform two types of comparison for the e–e case and for the e–i case. For the first type of comparisons, we keep the number of particles N at a constant value and compare the numerical results at different time steps

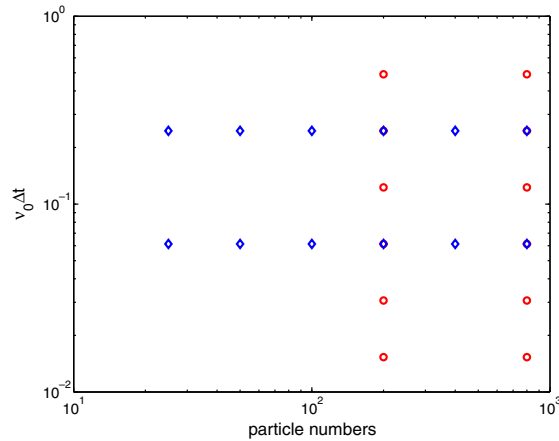


Fig. 2. $v_0\Delta t$ and N combinations.

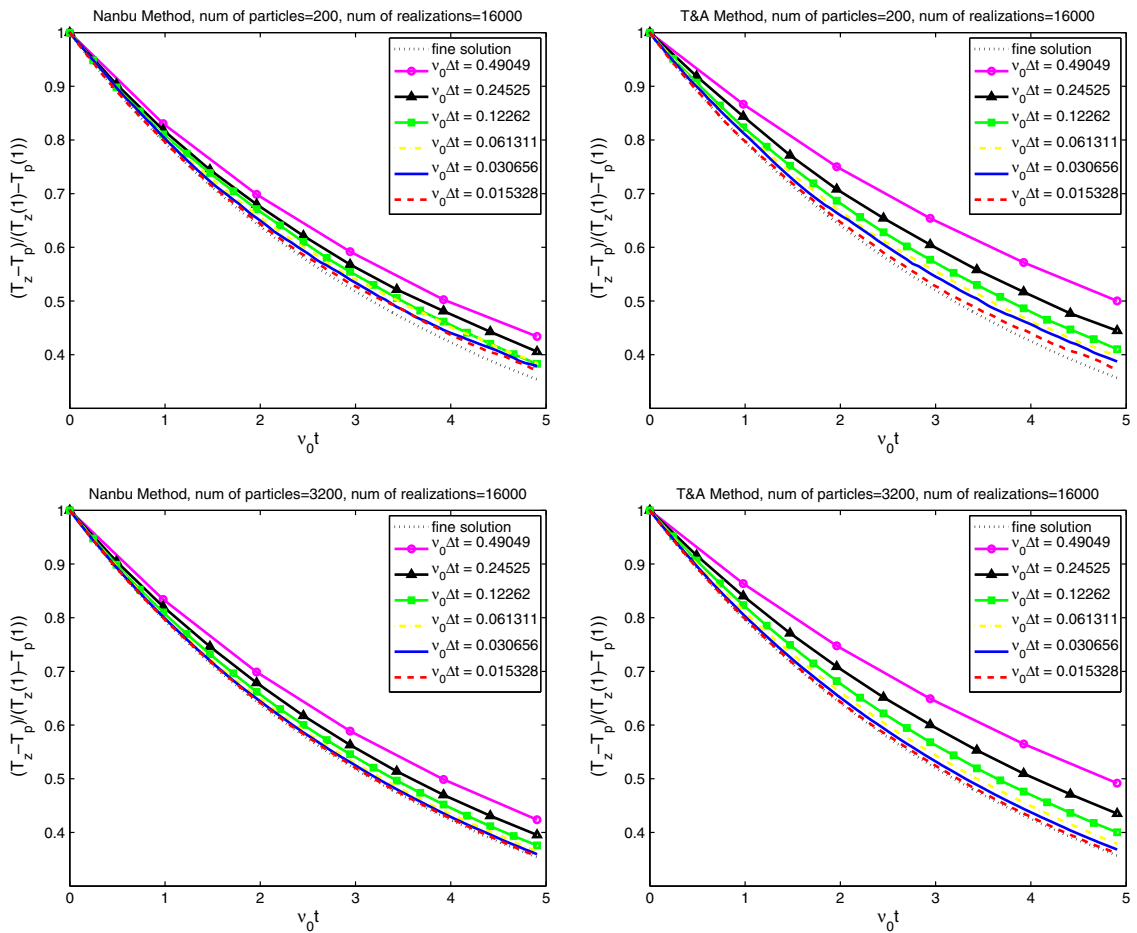


Fig. 3. (e–e case) Average solutions \bar{u} ; the results using Nanbu’s method are depicted in the left-hand column; results using TA’s method are shown in the right-hand column. In each graph, the top row results are computed using $N = 200$ particles and the bottom row results use $N = 3200$; average of 16,000 independent realizations.

Δt . This comparison enables us to see how changes in time step Δt will affect the accuracy of the simulation solutions. In the second comparison, we keep the time step Δt constant and vary the number of particles N in

the simulation. This enables us to see how changes in particle number N will affect the accuracy of the simulation solutions. We also perform more than one set of simulations for each type of comparison. For example, we perform simulations with $N = 200$ and 3200 , and for each N we perform simulation at various Δt , see Fig. 2. This way we can see the effects of N on the simulation results over different Δt 's.

In the e–i case the ions are loaded as an isotropic Maxwellian with mass ratio $m_i/m_e = 100$, charge ratio $e_i/e_e = -1$, and with $T_i = (T_x + T_y + T_z)/3$. Electron–ion collisions isotropize the initially anisotropic electron distribution at a rate that is similar to that for electron–electron collisions, however, the e–i collision differs physically. The electron–ion collisions are dominated by pitch-angle scattering for $m_i/m_e \gg 1$, while in e–e collisions the angle scattering, drag, and energy diffusion are competitive. For an ion temperature similar to the electron temperature, the ion velocities are much smaller than the electron velocities by $O(\sqrt{m_i/m_e})$. As a consequence, for purposes of the scattering of the electrons on the ions, the statistical requirements on the much slower ion velocity distribution are much less than on the electrons in the electron–electron collisions. Furthermore in our simulations there are either $N/2$ electron pairs (*i.e.*, N electrons) undergoing e–e collisions or N electron–ion pairs (*i.e.*, N electrons and N ions) undergoing e–i collisions. Thus, the magnitude of the statistical errors for the simulations with e–i collisions should be significantly less than those for the simulations with e–e collisions; and this is observed.

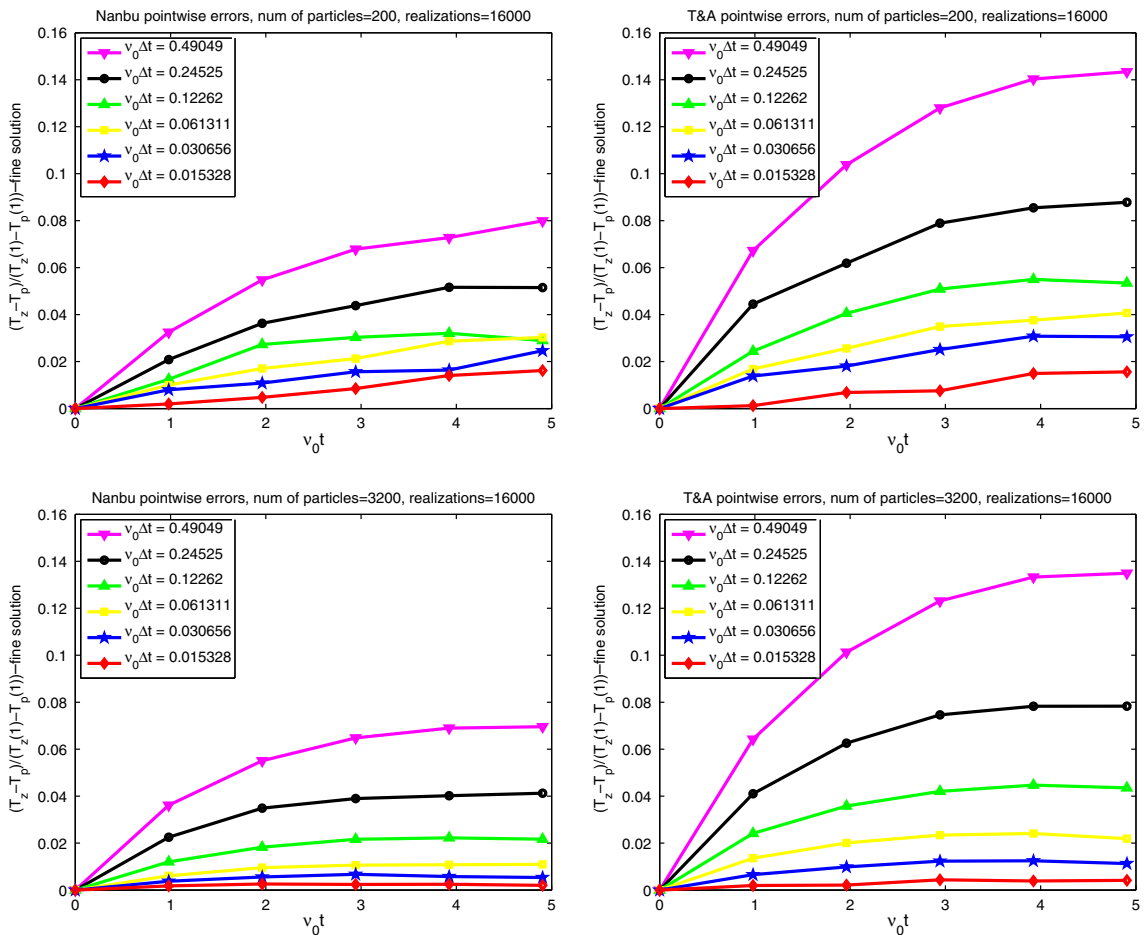


Fig. 4. (e–e case) Deterministic errors e_D ; the results using Nanbu’s method are depicted in the left-hand column; results using TA’s method are shown in the right-hand column. In each graph, the top row results are computed using $N = 200$ particles and the bottom row results using $N = 3200$; average of 16,000 independent realizations.

To separate the effects of the statistical fluctuations from the deterministic errors, we compute the mean and variance of M independent solutions. We call the average of such M independent realizations the deterministic solution \bar{u}

$$\bar{u}(\Delta t, N) = \frac{1}{M} \sum_{i=1}^M u_i$$

where $u_i = u_i(\Delta t, N)$ is the i th independent realization of the solution, and \bar{u} is the average of these independent realizations.

We designate $e_D(\Delta t, N)$ as the deterministic error when the time step is Δt and the number of particles is N . Specifically, let u_f be a numerical solution computed using a large number of particles and a small time step. An error $e_D(\Delta t, N)$ is defined as the difference between the average of M independent solutions computed using Δt and N and a fine solution u_f . In other words,

$$e_D(\Delta t, N, t) = |\bar{u}(\Delta t, N, t) - u_f(t)|.$$

The quantity $\sigma^2 = \sigma^2(\Delta t, N)$ represents the statistical fluctuations of the M independent solutions computed at a time step Δt and a number of particles N . σ^2 is defined by the empirical variance in the following way:

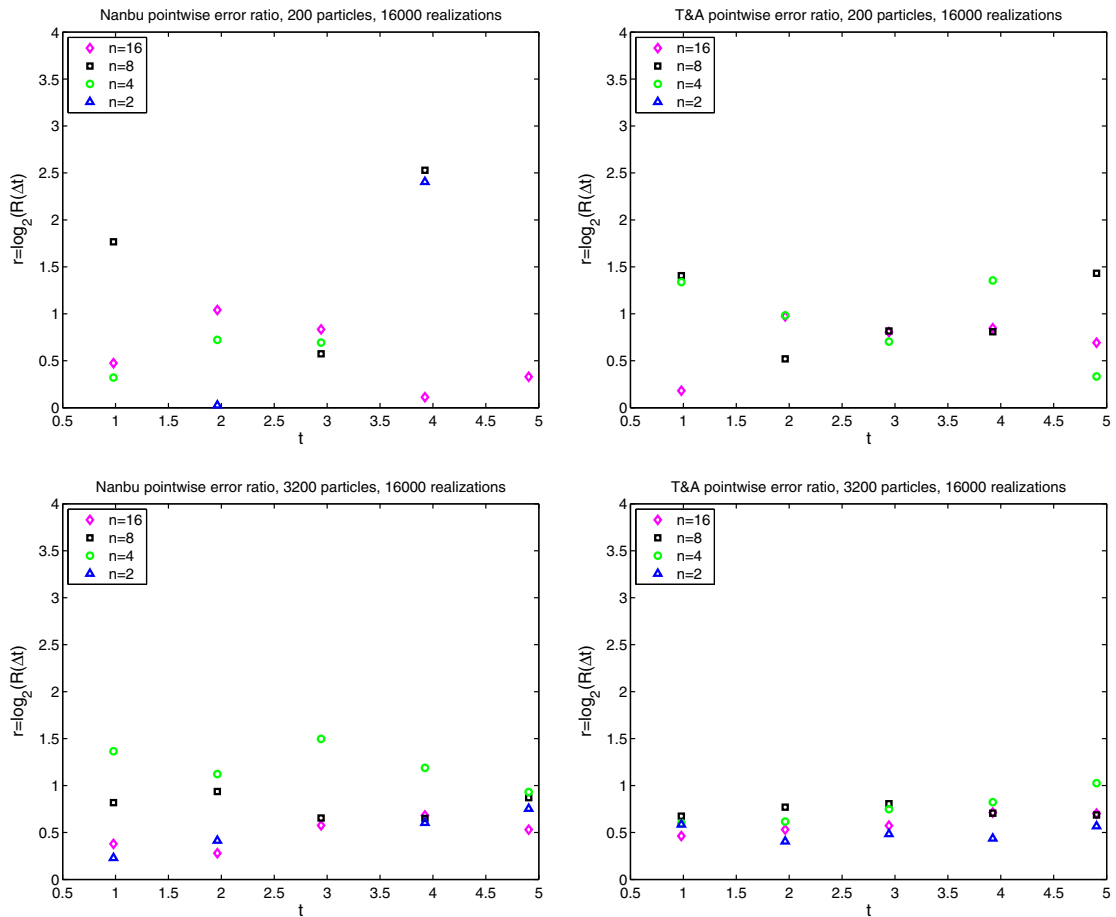


Fig. 5. (e–e case) Order of accuracy $r = \log_2 R(\Delta t)$; the results using Nanbu’s method are depicted in the left-hand column; results using TA’s method are shown in the right-hand column. In each graph, the top row results are computed using $N = 200$ particles and the bottom row results using $N = 3200$; average of 16,000 independent realizations.

$$\sigma^2(\Delta t, N) = \frac{1}{M} \sum_{i=1}^M (u_i - \bar{u})^2.$$

Hence $\sigma^2(\Delta t, N)$ represents the mean square deviation of the realizations u_i from the average solution \bar{u} .

To compute the order of accuracy with respect to time step Δt , we first compute the error ratio $R(\Delta t)$

$$R(\Delta t) = \left| \frac{\bar{u}(4\Delta t) - \bar{u}(2\Delta t)}{\bar{u}(2\Delta t) - \bar{u}(\Delta t)} \right|.$$

Let u_0 be the exact solution, and assume the average solution \bar{u} has order of accuracy of r , i.e.,

$$\bar{u}(\Delta t) = u_0 + C(\Delta t)^r.$$

where C is a constant. Then

$$R(\Delta t) = 2^r$$

and therefore the order of accuracy r

$$r = \log_2 R(\Delta t).$$

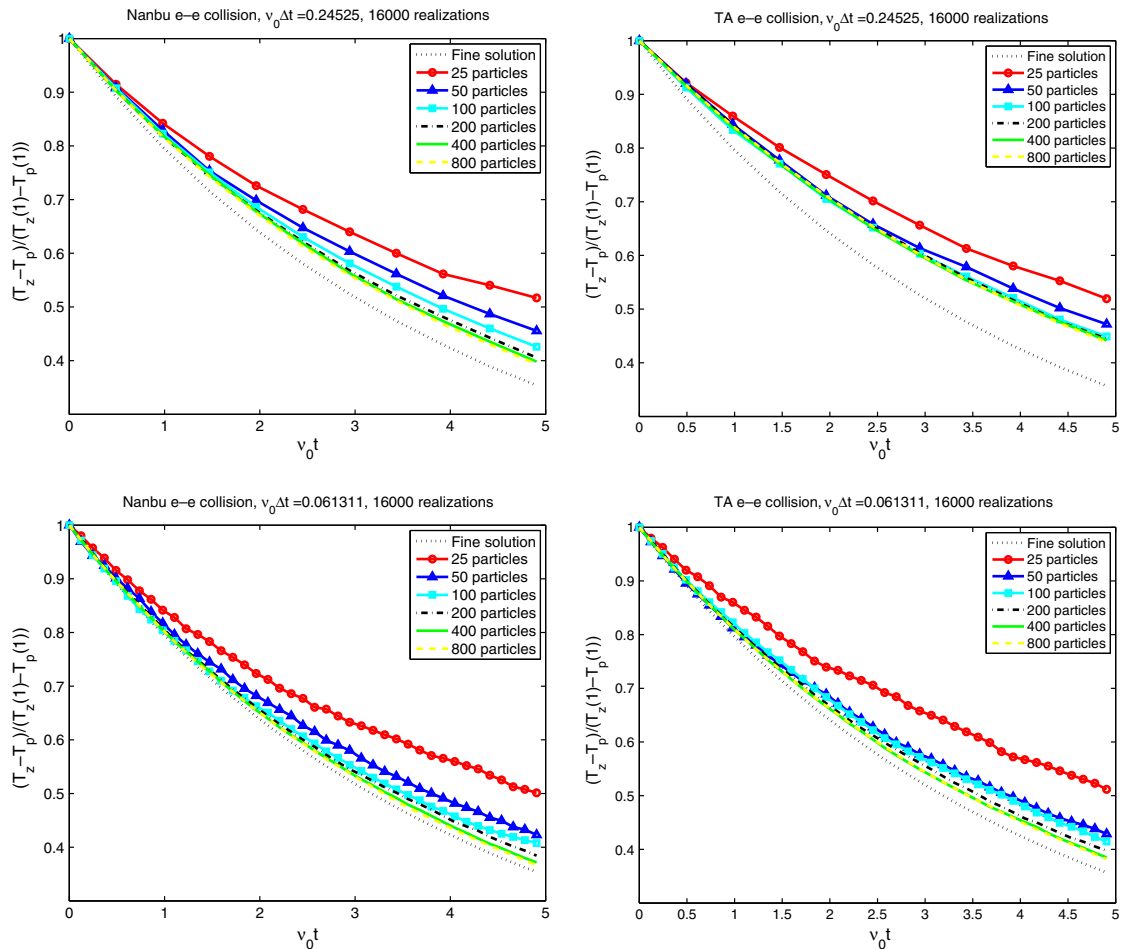


Fig. 6. (e–e case) Average solutions \bar{u} ; the results using Nanbu’s method are depicted in the left-hand column; results using TA’s method are shown in the right-hand column. In each graph, the top row results are computed using $v_0 \Delta t = 0.24525$, and the bottom row results using $v_0 \Delta t = 0.0613$.

For all the computations we present here, u_i represents the temperature difference between parallel direction T_z and perpendicular direction T_p normalized by the initial temperature difference.

$$u_i(t) = \frac{T_z(t) - T_p(t)}{T_z(0) - T_p(0)}$$

is used in the formulas above to define \bar{u} and u_r . In the computational results described in Section 4, we have used 16,000 independent simulations. These were divided into $M = 160$ groups of 100 simulations each with N particles. The temperatures T_z and T_p were computed by averaging over each group of 100 simulations to reduce the statistical errors. Then the average \bar{u} and the variance σ^2 were computed by averaging over the $M = 160$ groups.

4. Convergence results

The graphs of the computational results are described as below.

The first three plots show the simulation of deterministic solutions when N is constant, and Δt varies:

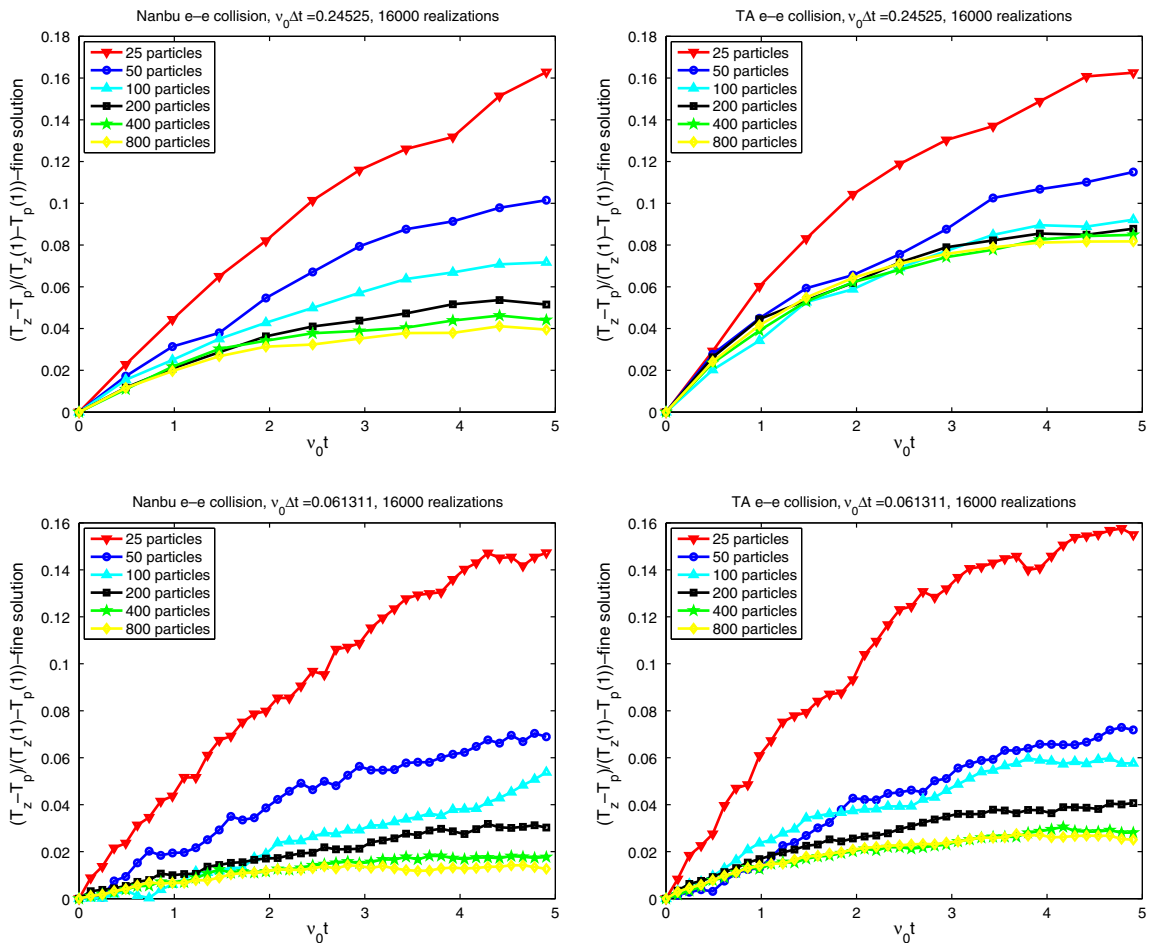


Fig. 7. (e–e case) Deterministic error e_D ; The results using Nanbu’s method are depicted in the left-hand column; results using TA’s method are shown in the right-hand column. In each graph, the top row results are computed using $v_0 \Delta t = 0.24525$, and the bottom row results using $v_0 \Delta t = 0.0613$.

- The average of 16,000 independent solutions is shown in Fig. 3 for e–e collisions and in Fig. 10 for e–i collisions. The independent simulations were used both to compute temperatures and to compute averages, as described at the end of Section 3.
- The pointwise errors are shown in Fig. 4 for e–e collisions and Fig. 11 for e–i collisions.
- The pointwise order of accuracy $r = \log_2 R(\Delta t)$ is shown in Fig. 5 for e–e collisions.

The next two plots show the deterministic solutions when Δt is constant, and N varies:

- The average of 16,000 independent solutions is shown in Fig. 6 for e–e collisions and Fig. 12 for e–i collisions.
- The deterministic pointwise errors e_D are shown in Fig. 7 for e–e collisions and Fig. 13 for e–i collisions.

The simulation of statistical fluctuations is shown in the following part of the graphs:

- Figs. 8 and 14 show the statistical fluctuations when N is constant and Δt varies for e–e collisions and e–i collisions, respectively.

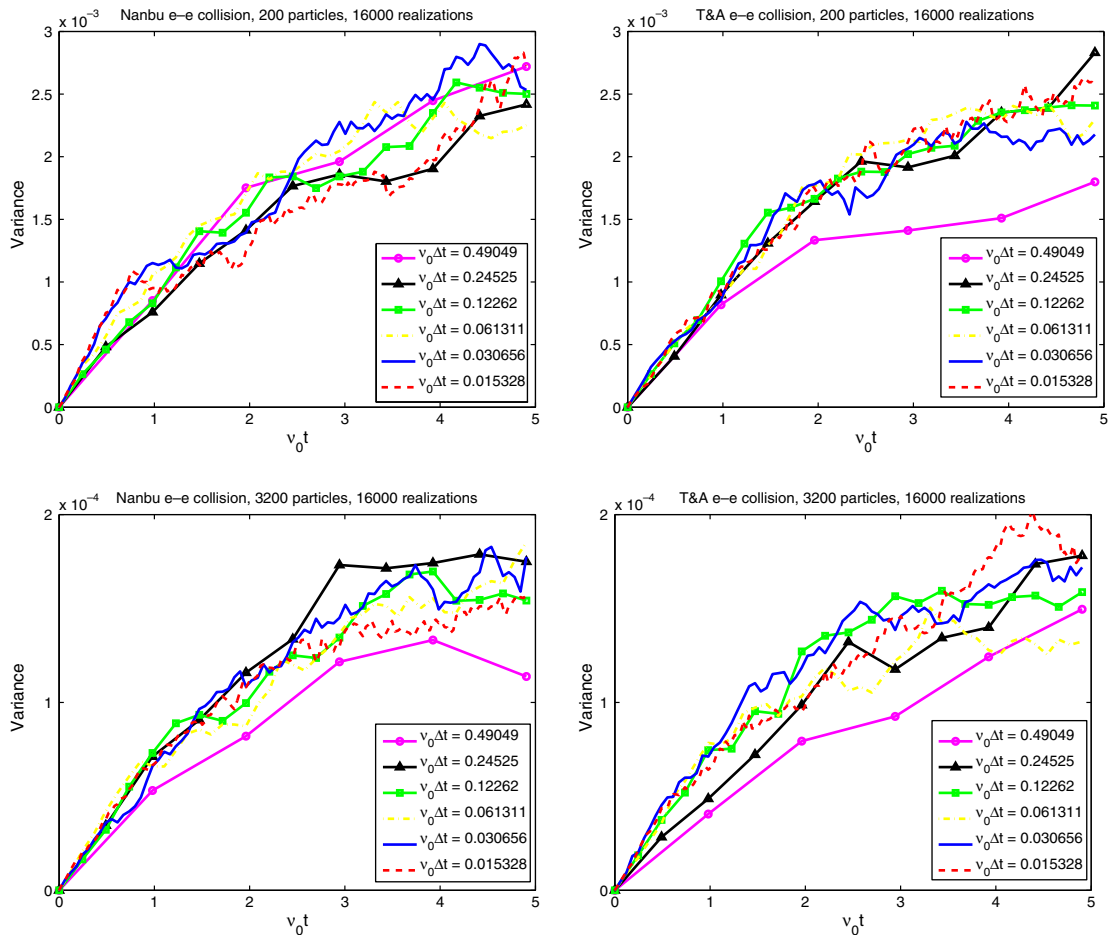


Fig. 8. (e–e case) Variance σ^2 of the results using Nanbu’s method are depicted in the left-hand column; results using TA’s method are shown in the right-hand column. In each graph, the top row results are computed using $N = 200$ particles and the bottom row results using $N=3200$; average of 16,000 independent realizations.

- Figs. 9 and 15 show the statistical fluctuations when Δt is constant and N varies for e–e collisions and e–i collisions, respectively.

The convergence results are presented in the following manner. We first present results computed using Nanbu’s method and then results computed using TA’s method. In the discussion about each method, we first describe the results of deterministic (*i.e.*, averaged) solutions. We show the simulations with a constant number of particles N and varying time step Δt , as well as constant Δt and varying N . In order to understand the order of time step accuracy, we also include the pointwise error ratio r . We then explain the results of statistical fluctuations with the same set of Δt and N combinations as the deterministic case.

For all the plots presented here, the computational results obtained using Nanbu’s method are shown in the left-hand column, whereas results obtained using TA’s method are represented in the right-hand column.

To analyze the Δt convergence for TA or Nanbu’s method, we generate a fine solution u_f for each method. The fine solutions are obtained using 6,400 particles and $v_0\Delta t = 0.0076$, where v_0 is the effective collision frequency. We use individual fine solution for each method to exclude the possibility of systematic errors for Δt convergence. However, the difference of the two fine solutions is very small. We note that the simulations exhibit convergence when Δt and $1/N$ are small. The deterministic error due to Δt and the statistical error due to N both contribute to the total error in the solutions. For fixed N as Δt is decreased the errors in the simulations

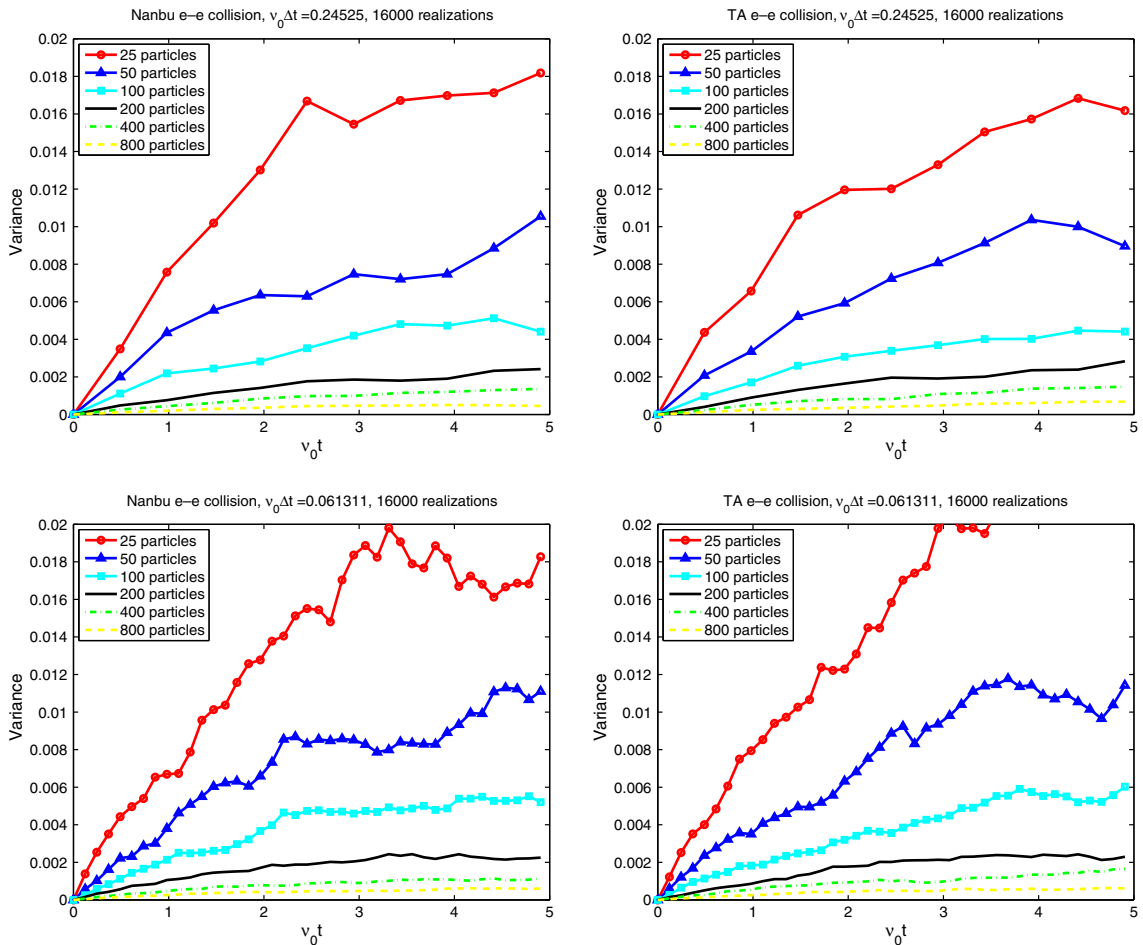


Fig. 9. (e–e case) Variance σ^2 of the results using Nanbu’s method are depicted in the left-hand column; results using TA’s method are shown in the right-hand column. In each graph, the top row results are computed using $v_0\Delta t = 0.24525$, and the bottom row results using $v_0\Delta t = 0.0613$.

decrease monotonically until the statistical errors are dominant, and further decreases in Δt are ineffective in reducing the total error. Similarly, for fixed Δt increasing N decreases the total error until N is sufficiently large that further increases in N smooth the total error but are ineffective in reducing it.

After completing the scan of Δt for fixed N , we realized that with the number of collisions per particle per time step fixed, increasing Δt had the effect of reducing the number of random numbers sampled in computing the collisions per unit time. Because the statistical errors arise from both the number of particles used to resolve the velocity distribution and the number of random numbers used to represent the collisions, the effect of increasing the time step was to reduce N_R , the number of random numbers, by a factor proportional to $1/\Delta t$. With a contribution to the statistical errors scaling as $1/\sqrt{N_R}$, the series of simulations scanning Δt introduced a statistical error growing with increasing time step as $\sqrt{\Delta t}$. Our data showing the results of the Δt scan are in some qualitative agreement with this scaling argument (Fig. 5). By holding the number of collisions per particle per time step fixed while increasing the size of the time step, the TA and Nanbu’s method conflated the effects of Δt and the statistics of sampling the random numbers on the results of the simulations of collisional relaxation.

In contrast to increasing Δt with fixed N , if we modify the TA and Nanbu methods by increasing the number of collisions per particle per time step $N_{\text{coll-p}}$ along with Δt so that the ratio of $\Delta t/N_{\text{coll-p}}$ is constant, then the collisional scattering is essentially unchanged from not having changed Δt and $N_{\text{coll-p}}$ at all (assuming that there is no particle advection or acceleration in fields). This was confirmed in a series of simulations. Clearly

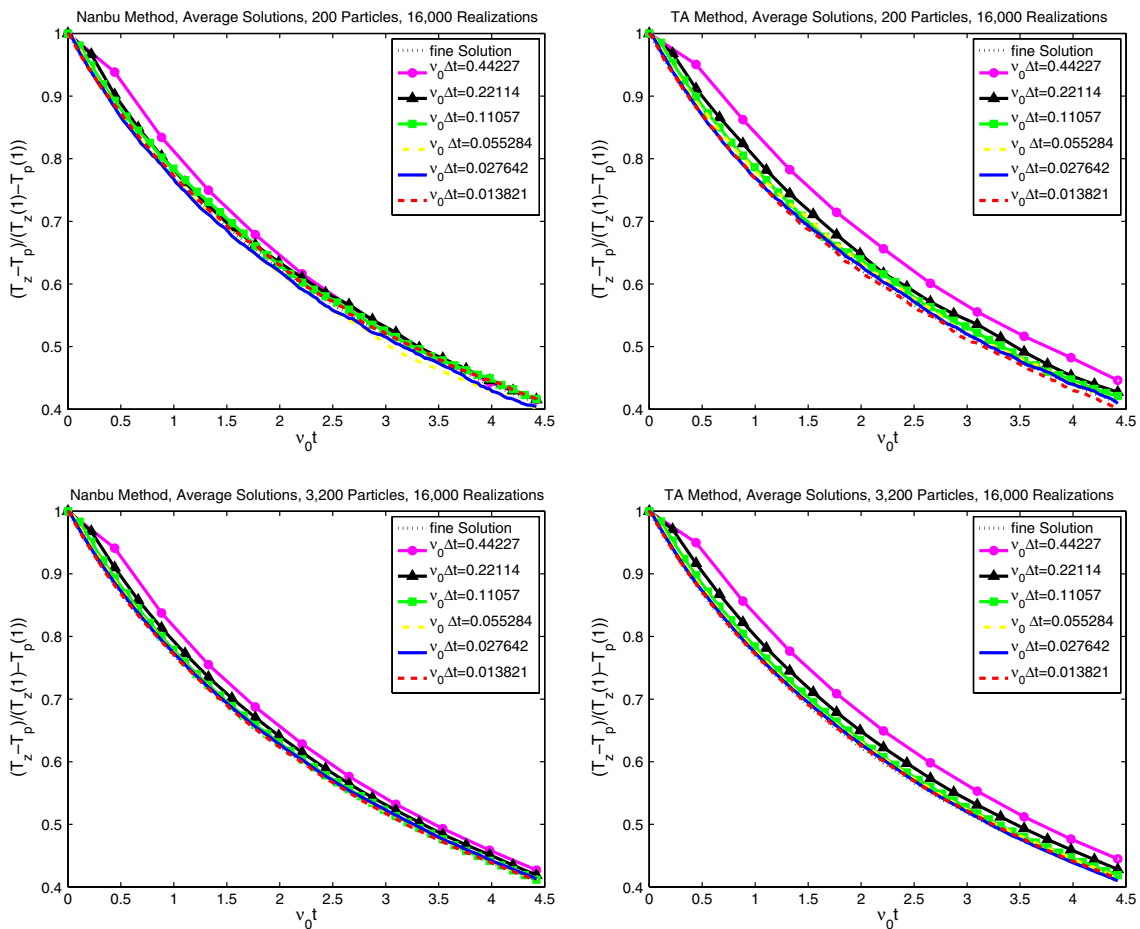


Fig. 10. (e–i case) Average solutions \bar{u} ; the results using Nanbu’s method are depicted in the left-hand column; results using TA’s method are shown in the right-hand column. In each graph, the top row results are computed $N = 200$ particles and the bottom row results using $N = 3200$; average of 16,000 independent realizations.

separating deterministic effects due to Δt from the statistical effects arising from changing the number of collision events and samples from the distribution of random numbers used in the collision operator is not trivial.

4.1. Simulation results using Nanbu’s method

In this section, we present the simulation results using Nanbu’s model. We discuss both the e–e and the e–i cases.

4.1.1. Deterministic solutions $\bar{u}(\Delta t, N, t)$ and errors $e_D(\Delta t, N)$

We begin with the deterministic solutions \bar{u} , when N is held constant and equal to 200 and 3200 and Δt varies, see Fig. 3 for the e–e case and Fig. 10 for the e–i case. It is evident that random fluctuations from the Monte Carlo simulation are eliminated after computing the average solutions, resulting in smooth time relaxation curves \bar{u} . Clearly, when the time step Δt is smaller, simulation solutions approach the fine solution u_f . Additionally, if the number of particles is increased, we also see an improvement in accuracy. Fig. 4 (e–e) and Fig. 11 (e–i) shows the result that when we keep N constant, $e_D(\cdot, N)$ decreases as Δt becomes smaller. When an e–e simulation was run longer, the error as shown in Fig. 4 peaks at a later time and then decreases. This qualitative behavior resembles that seen in Fig. 11 for the e–i cases. We note that the general level of errors in Fig. 11 for the e–i collisions is significantly smaller than the corresponding errors for e–e collisions

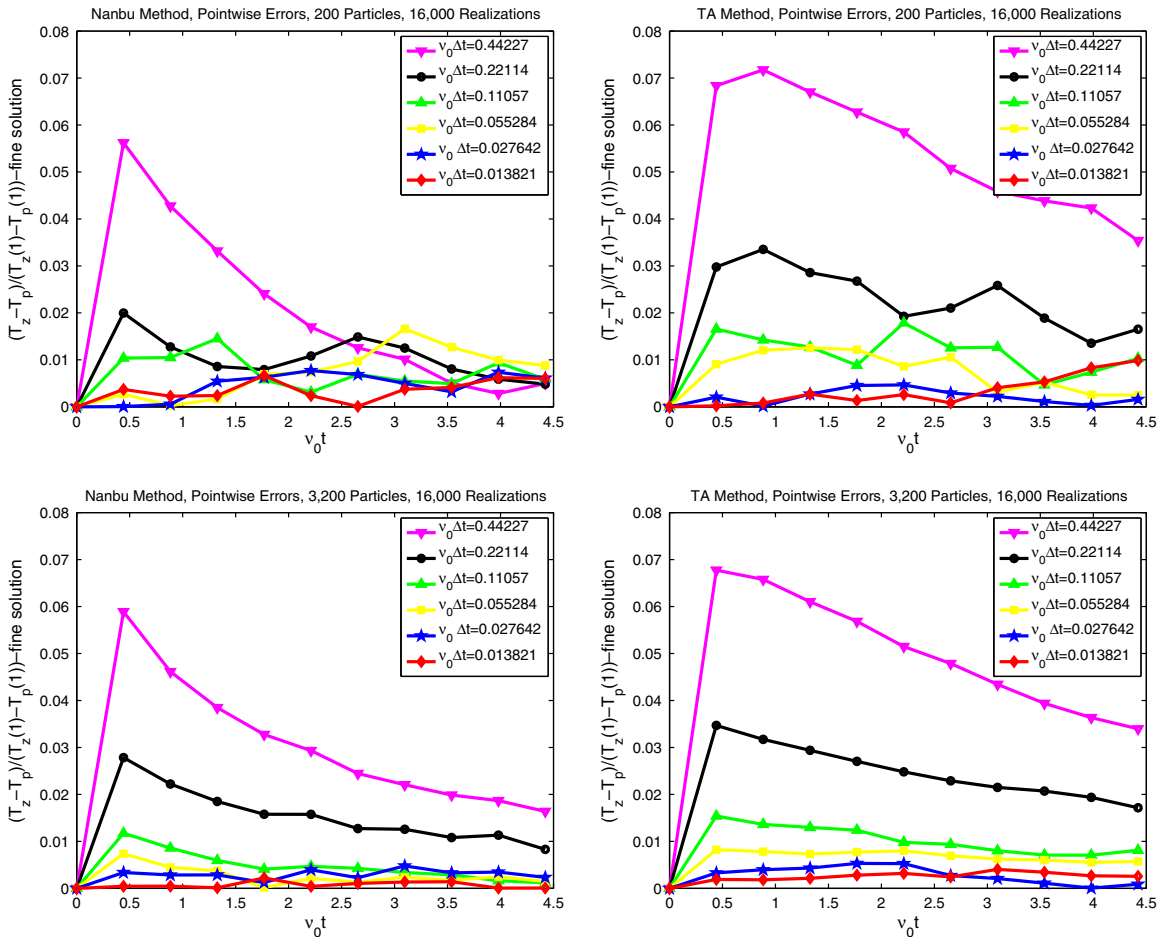


Fig. 11. (e–i case) Deterministic errors e_D ; the results using Nanbu’s method are depicted in the left-hand column; results using TA’s method are shown in the right-hand column. In each graph, the top row results are computed using $N = 200$ particles and the bottom row results using $N = 3200$; average of 16,000 independent realizations.

shown in Fig. 4 in keeping with our earlier arguments based on the superior statistical resolution of the e–i collisional simulations. To see the order of accuracy, we compute the order of accuracy $r = \log_2 R(\Delta t)$. In the e–e case, Nanbu’s method does not produce a precise order of accuracy but rather oscillates around the value $r = 0.5$, see Fig. 5. In the e–i case, we could not reach a conclusion about the order of accuracy, see Fig. 16.

When Δt is held constant and N increases, the results for the e–e and the e–i cases are relatively different. In the e–e case, the average solutions approach the fine solution u_f , see Fig. 6. The corresponding pointwise errors $e_D(\Delta t, \cdot)$ of the average solutions \bar{u} are depicted in Fig. 7. For each constant time step Δt , $e_D(\Delta t, \cdot)$ decreases linearly as the number of particles N increases. In other words, the order of accuracy for the number of particles is $O(N^{-1})$. Moreover, as might be expected, for any number of particles N , $e_D(N, \Delta t = 0.0613/v_0)$ is less than $e_D(N, \Delta t = 0.24525/v_0)$. In the e–i case, we see generally the errors $e_D(\Delta t, N)$ decrease when the number of particles N increases, but the result is not as clearcut as the e–e case, see Figs. 12 and 13. We note that the error at the first time step can be large, and there is no error at t_0 by construction. The largest errors at the first time step coincide with the largest values of $v_0\Delta t$ used, which are so large that the numerical collision operator cannot compute the small-angle scattering accurately for a significant fraction of the velocity distribution. The error at the first time step decreases significantly as $v_0\Delta t$ becomes small. As time progresses in the simulation, the angle scattering (although inaccurate at large values of $v_0\Delta t$) relaxes the initial anisotropy toward zero.

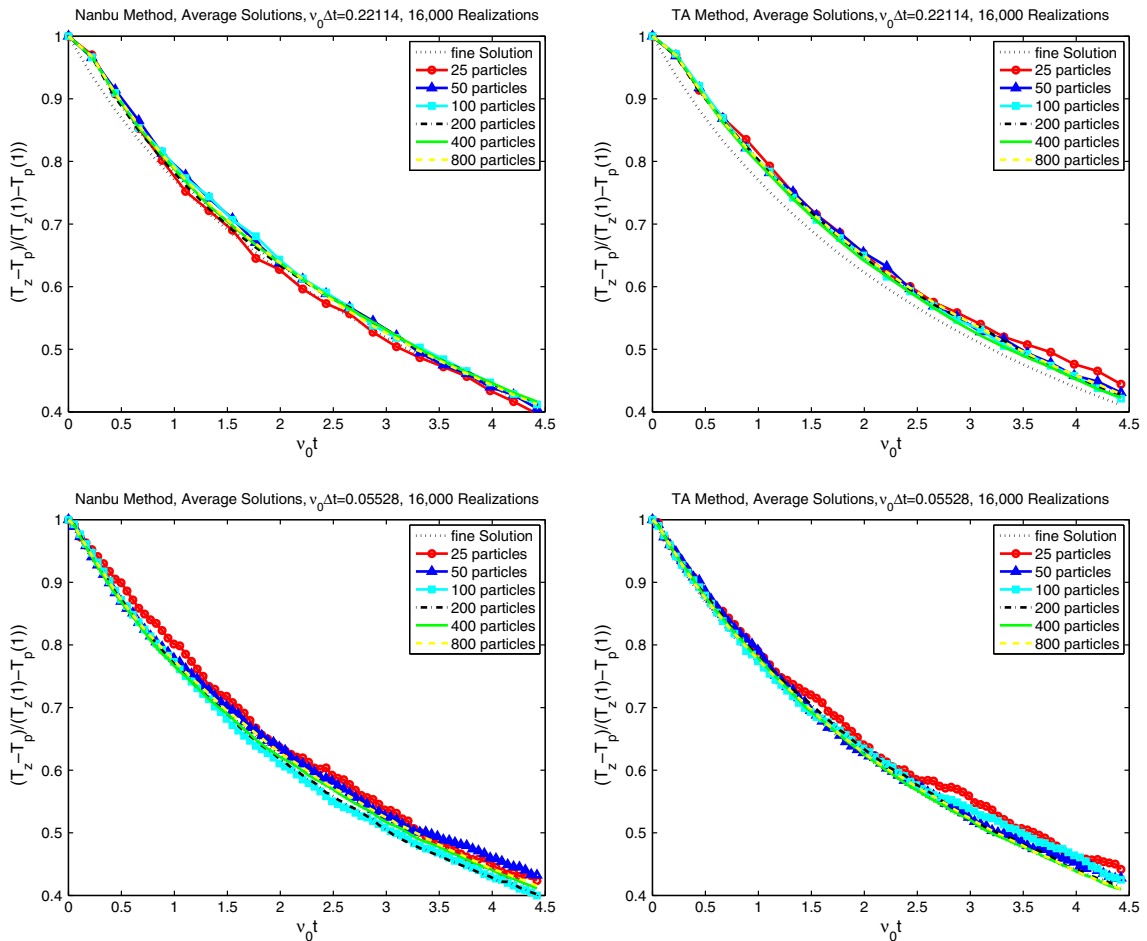


Fig. 12. (e–i case) Average solutions \bar{u} ; the results using Nanbu’s method are depicted in the left-hand column; results using TA’s method are shown in the right-hand column. In each graph, the top row results are computed using $v_0\Delta t = 0.2211$, and the bottom row results using $v_0\Delta t = 0.05528$.

Because the anisotropy in the fine solution relaxes to zero as time progresses, the error in the anisotropy in the simulation with respect to the fine solution necessarily also relaxes toward zero after the first time step (the difference of two quantities both going to zero). Thus, the error at the first time step for large $v_0\Delta t$ is most pronounced in the time histories of the errors.

4.1.2. Statistical fluctuations $\sigma^2(\Delta t, N)$

The numerical solutions computed using the Monte Carlo method are composed of deterministic components and statistical fluctuations. In order to completely understand the statistical accuracy of the solutions, we analyze the statistical fluctuations σ^2 of the solutions.

We first calculated the statistical fluctuations $\sigma^2(\cdot, N)$ at various time steps Δt for $N = 200$ and 3200 and 16,000 realizations. From Fig. 8 (e–e case) and Fig. 14 (e–i case) we can see that for each constant N , statistical fluctuations $\sigma^2(\cdot, N)$ have approximately the same values and are independent of the time steps Δt 's. In other words, reducing the time step Δt does not have any influence on $\sigma^2(\cdot, N)$.

We then compute $\sigma^2(\Delta t, \cdot)$ when the time step Δt is held constant. The time step $v_0\Delta t$ in the e–e case is equal to 0.2452 and 0.06013, and $v_0\Delta t$ in the e–i case is 0.22214 and 0.05528, see Fig. 9 (e–e case) and Fig. 15 (e–i case). The statistical fluctuations $\sigma^2(\Delta t, \cdot)$ decreases linearly as the number of particles N increases. This means that the order of particle number accuracy is $O(N^{-\frac{1}{2}})$, and one can reduce random fluctuations by increasing the number of particles N , as is commonly expected.

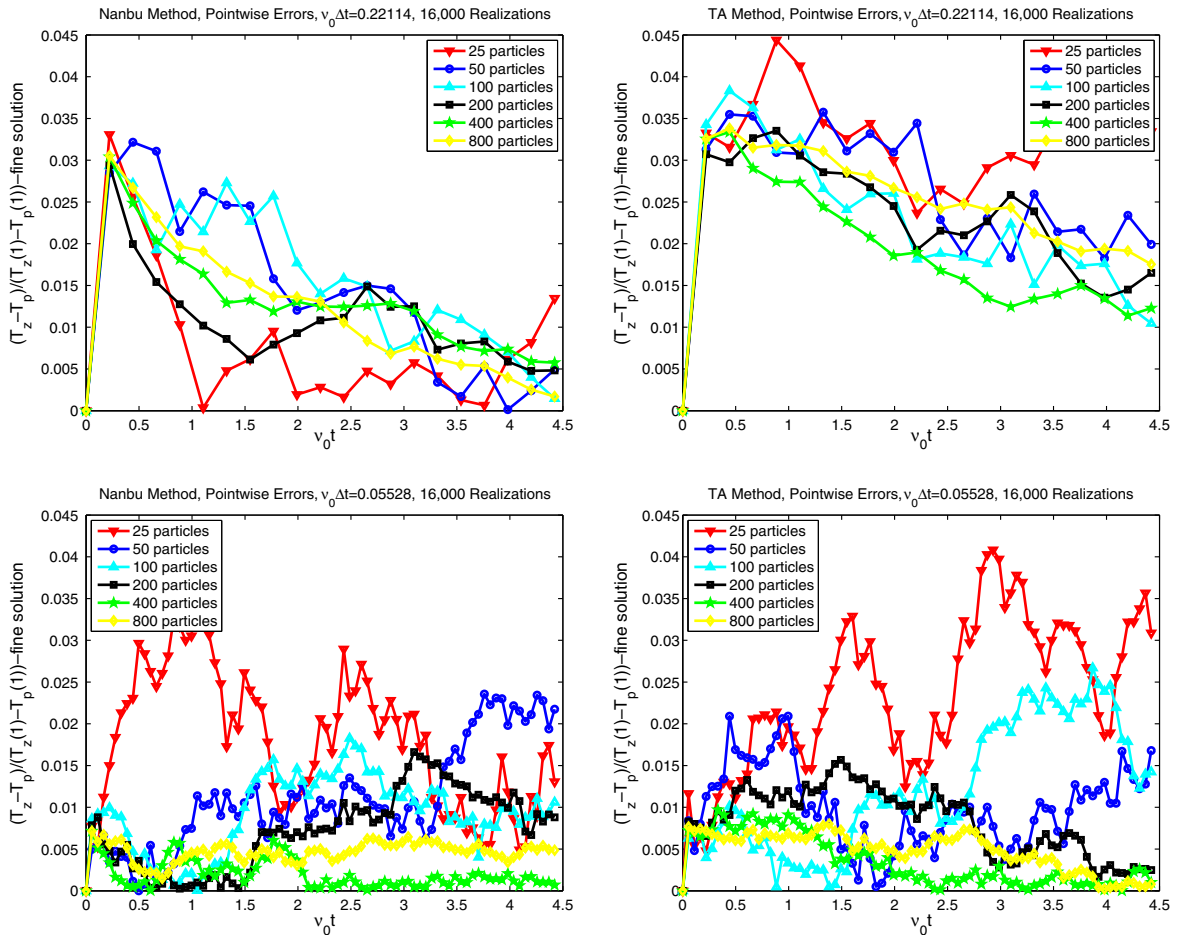


Fig. 13. (e–i case) Deterministic error e_D ; the results using Nanbu’s method are depicted in the left-hand column; results using TA’s method are shown in the right-hand column. In each graph, the top row results are computed using $v_0\Delta t = 0.2211$, and the bottom row results using $v_0\Delta t = 0.05528$.

4.2. Simulation results using TA's method

In this section, we describe the computational results obtained using TA's method. We perform exactly the same computations as for Nanbu's model. This requires determining the average solutions \bar{u} and errors e_D and statistical fluctuation σ^2 at various time steps Δt and number of particles N .

4.2.1. Deterministic solutions $\bar{u}(\Delta t, N, t)$ and errors $e_D(\Delta t, N)$

We use the same procedure as we used with Nanbu's method. Specifically, we compute the average of 16,000 independent solutions when the number of particles N are held constant and equal to 200 and 3200, see Fig. 3 for the e–e case and 10 for the e–i case. The average solutions eliminate random fluctuations from the Monte Carlo simulation, resulting in smooth time relaxation curves \bar{u} . When the time step Δt is smaller, simulation solutions approach the fine solution u_f . If the number of particles is increased, we also see an improvement in accuracy. Fig. 4 (e–e case) and Fig. 11 (e–i case) shows that when we keep N constant, $e_D(\cdot, N)$ decreases as Δt becomes smaller. When an e–e simulation was run longer, the error as seen in Fig. 4 peaks at a later time and then decreases. This qualitative behavior resembles that seen in Fig. 11 for the e–i cases.

When Δt is held constant, \bar{u} approaches the fine solution u_f as N increases, as shown in Fig. 6 (e–e case) and Fig. 12 (e–i case), however, the results for e–e and e–i cases are again different. In the e–e case, the

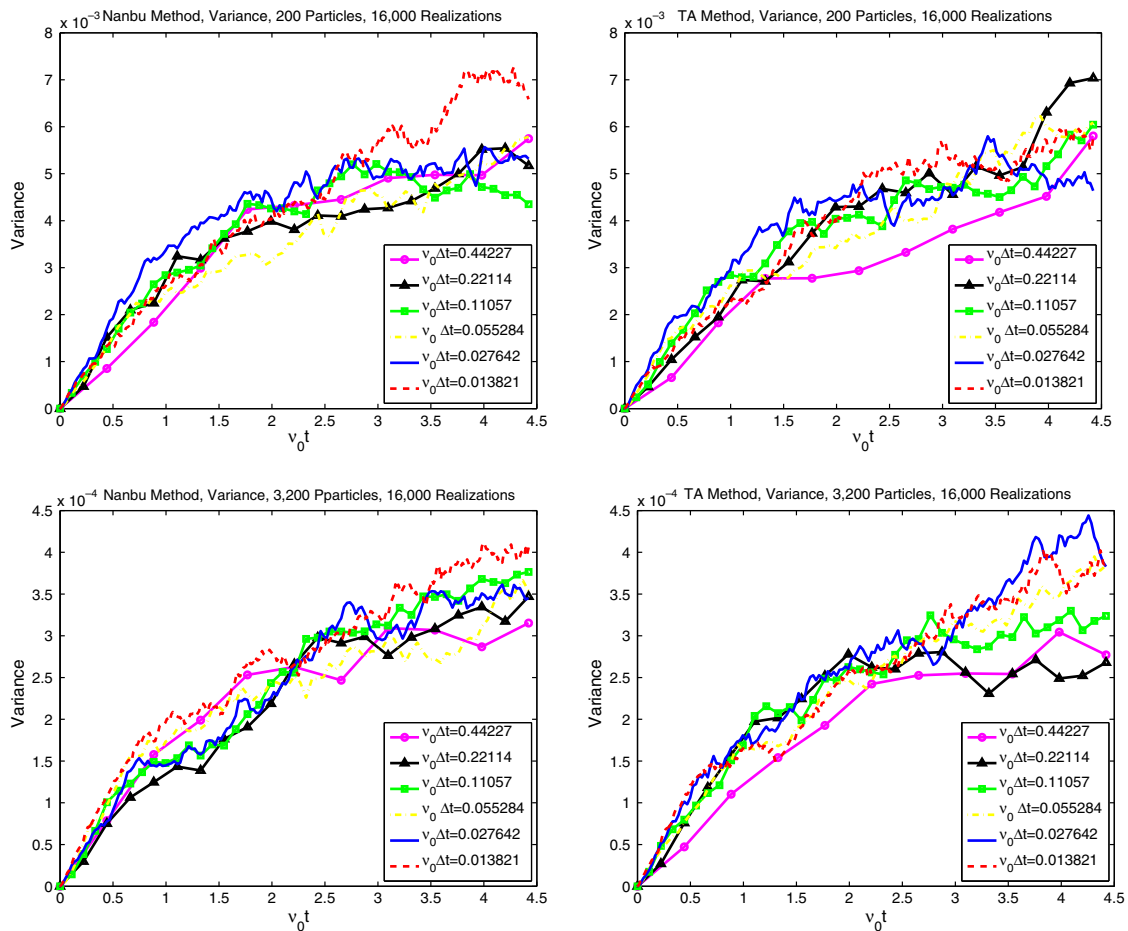


Fig. 14. (e–i case) Variance σ^2 of the results using Nanbu's method are depicted in the left-hand column; results using TA's method are shown in the right-hand column. In each graph, the top row results are computed using $N = 200$ particles and the bottom row results using $N = 3200$; average of 16,000 independent realizations.

corresponding pointwise errors $e_D(\Delta t, \cdot)$ decreases linearly as the number of particles N increases, see Fig. 7. For any number of particles N , $e_D(N, \Delta t = 0.0613/v_0)$ is smaller than $e_D(N, \Delta t = 0.24525/v_0)$. In the e–i case, overall the errors $e_D(\Delta t, N)$ decrease when the number of particles N increases, and $e_D(N, \Delta t = 0.05528/v_0)$ is generally smaller than $e_D(N, \Delta t = 0.2211/v_0)$, but the result is not as distinct as the e–e case, see Fig. 13.

TA’s method in the e–e case yields a clear value of order $r = 0.5$ when the number of particles $N = 3200$, as shown in Fig. 5. However, we cannot obtain the order of accuracy r through error ratio in the e–i case, as shown in Fig. 16.

In general Δt has to be small enough to see any improvement in accuracy when the number of particles N increases. If Δt is too large, the time step errors dominate, and no improvement of accuracy will occur when N increases. Fig. 7 also shows the relation between time step errors and particle number errors for the e–e case. When $v_0\Delta t = 0.24525$, we can not reduce the errors e_D by increasing the number of particles N . For the e–i case, the corresponding results are not so clear. There is some decrease in the error with increasing N only for the smaller value of the time step. We note that the errors in the e–i case in Fig. 13 are significantly smaller than those in Fig. 7 because the statistical requirements for the e–i case are weaker. We point out that the error at the first time step is large for large $v_0\Delta t$ because of the same reason as discussed in the Nanbu’s case in Section 2.1.

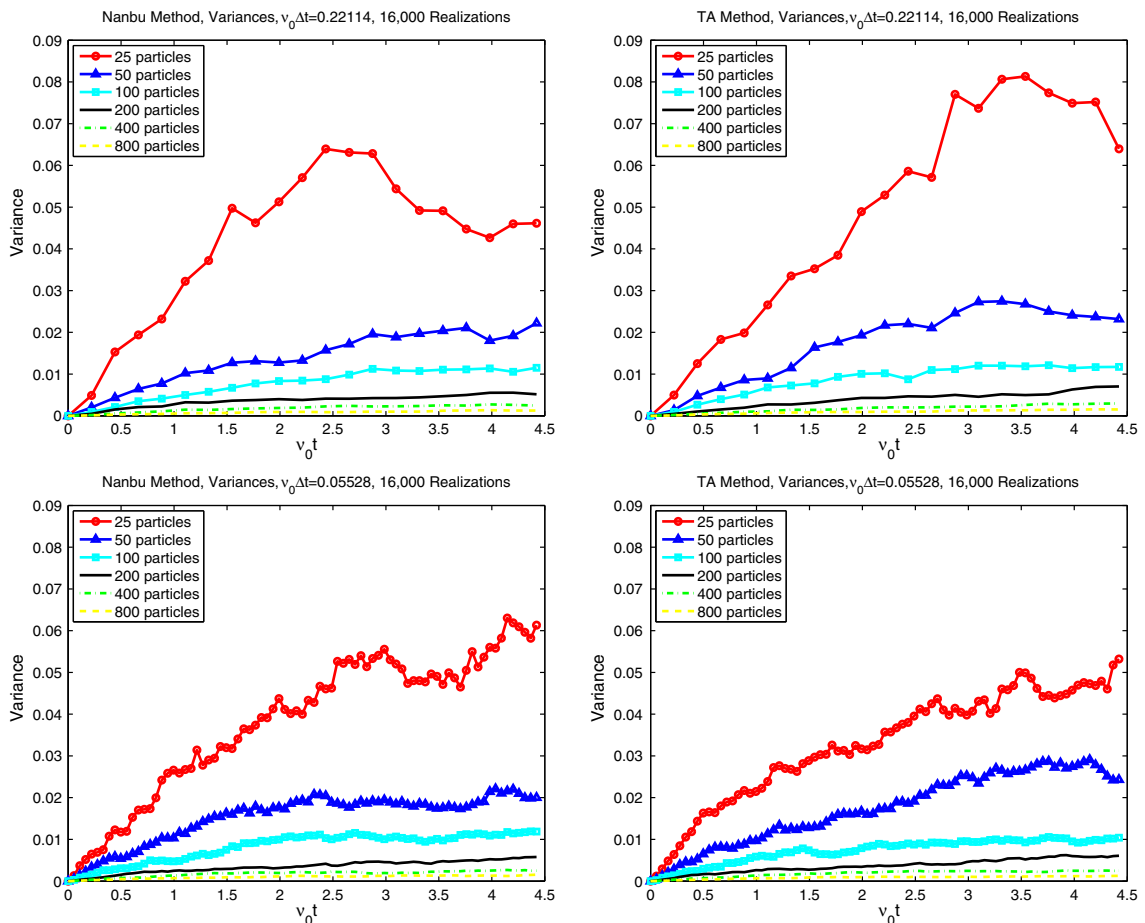


Fig. 15. (e–i case) Variance σ^2 of the results using Nanbu’s method are depicted in the left-hand column; results using TA’s method are shown in the right-hand column. In each graph, the top row results are computed using $v_0\Delta t = 0.2211$, and the bottom row results using $v_0\Delta t = 0.05528$.

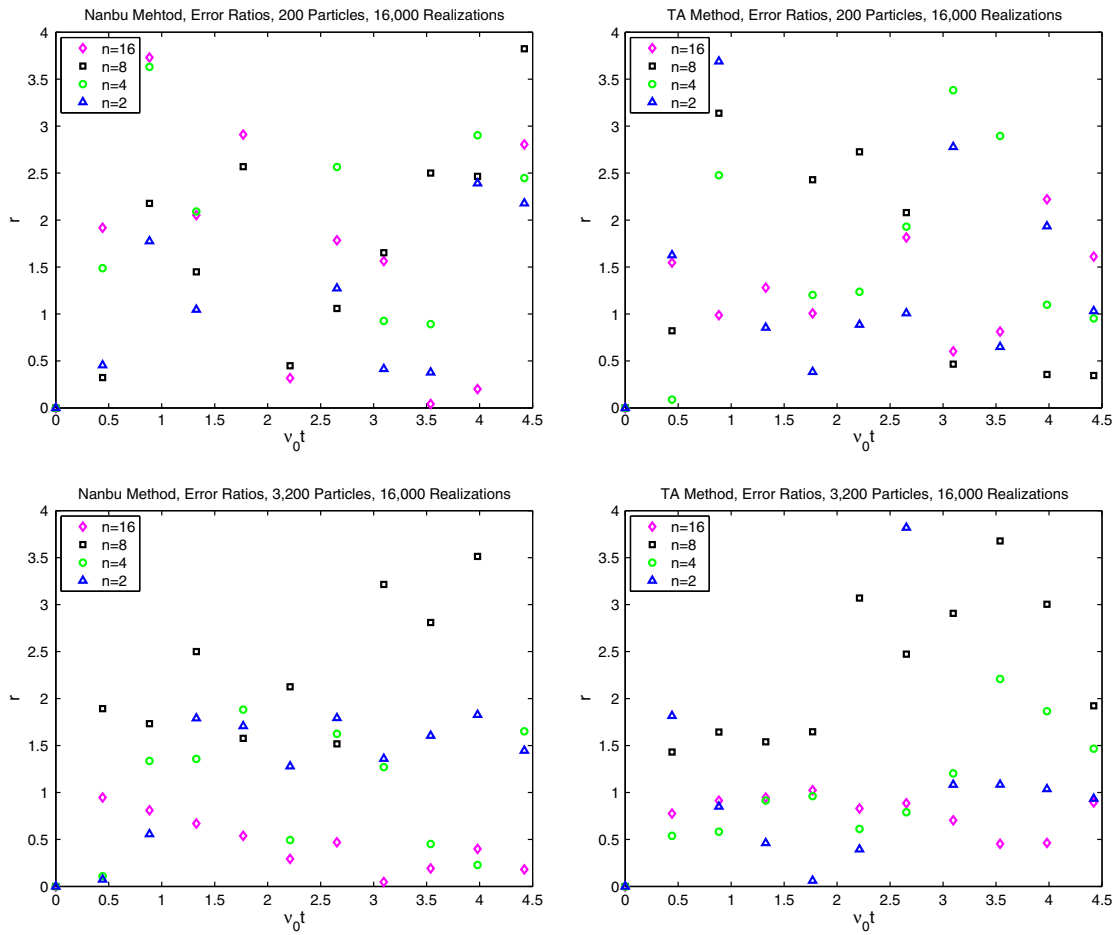


Fig. 16. (e–i case) Order of accuracy $r = \log_2 R(\Delta t)$; the results using Nanbu’s method are depicted in the left-hand column; results using TA’s method are shown in the right-hand column. In each graph, the top row results are computed using $N = 200$ particles and the bottom row results using $N = 3200$; average of 16,000 independent realizations.

4.2.2. Statistical fluctuations $\sigma^2(\Delta t, N)$

The numerical solutions computed using the Monte Carlo method have deterministic components and statistical fluctuations. We examine the statistical fluctuations σ^2 of the solutions in this section. We again calculate the statistical fluctuations $\sigma^2(\cdot, N)$ at various time steps Δt for $N = 200$ and 3200. The e–e case and the e–i case produce similar results. We observe that for each constant N , statistical fluctuations $\sigma^2(\cdot, N)$ have approximately the same values and are independent of the time steps Δt ’s, as shown in Figs. 8 and 14. Evidently, reducing the time step Δt does not have significant effect on $\sigma^2(\cdot, N)$. The fluctuations are independent of the time step Δt .

Once again we compute $\sigma^2(\Delta t, \cdot)$ when $v_0 \Delta t$ is kept fixed and is equal to 0.2452 and 0.06013, see Figs. 9 and 15. The statistical fluctuations $\sigma^2(\Delta t, \cdot)$ diminish linearly as the number of particles N grows. This means when the time step Δt is constant, the fluctuations decrease like $O(N^{-\frac{1}{2}})$.

4.3. Comparison of the two methods

Simulation results obtained using the TA’s model were actually very similar to Nanbu’s model in the e–e case and e–i case. Both methods yield more conclusive results in the e–e case than the e–i case. The major advantage of Nanbu’s method is that the results are more accurate in terms of deterministic errors e_D . Specifically, it yields approximately half the pointwise errors $e_D(\Delta t, N)$ compared to TA’s method, see Fig. 4

$$e_{\text{DNanbu}}(\Delta t, N) \approx \frac{1}{2} e_{\text{DTA}}(\Delta t, N).$$

However, as discussed in previous sections of this article, Nanbu's method does not yield a higher order of accuracy r . Using TA's method we obtain a clearly defined r equal to 0.5, whereas the order of accuracy r for Nanbu's method oscillates around 0.5 in the e–e case, as shown in Fig. 5. The statistical fluctuations σ^2 for both methods decrease linearly as N increases, as shown in Fig. 9. However, when the particle number N is held constant, the statistical fluctuations are independent of the time step Δt , and using both methods results in approximately the same fluctuations, see Fig. 8. In other words,

$$\sigma^2(\Delta t, N) \approx cN^{-1}$$

where c is independent of N and Δt and is applicable to both Nanbu and TA's methods. As we have pointed out, two error sources, from time step and number of particles, exist in the simulation. One can see the relation between time step errors and particle number errors for both methods from Fig. 7. To see any improvement in accuracy when the number of particles N increases, Δt has to be small enough so the major errors come from the number of particles N . From this point of view, Nanbu's method also has advantages over TA's method. One can use larger Δt , *i.e.*, $v_0\Delta t = 0.24525$ in the e–e case, and still see the improvement in accuracy when N increases. This also shows Nanbu's method produces smaller time step errors.

For the same time step and number of particles, Nanbu and TA take about the same time. Nanbu may be a bit slower because it involves inverting a function, but this problem can be resolved by computing A in advance and storing the result for quick access. One can also ask whether Nanbu's method is more accurate, so that it would be faster for fixed error tolerance. Our paper is aimed at answering that question, and the results are mixed: the statistical error is the same for the two methods, but the deterministic error is about two times smaller for Nanbu.

5. Summary and discussion

In this paper, we have performed a convergence analysis to compare the two widely-used Monte Carlo binary collision models proposed by Takizuka & Abe and Nanbu. Our test case is a spatially homogeneous plasma with no electric or magnetic fields. We compute the relaxation of anisotropic temperatures over time due to collisions, using the results to evaluate the accuracy and efficiency of these two methods. Extensive simulation results are presented for both electron–electron and electron–ion collision cases. To facilitate the error analysis, we extract the deterministic errors by computing the mean of multiple statistically independent solutions. The statistical errors are computed using the empirical variance of these solutions. The comparison includes both the deterministic errors and statistical errors when the time step or number of particles is varied. We also compute the order of accuracy in time using an error ratio.

There are a number of similarities between the two methods. Both methods yield more conclusive results in the e–e case. In the e–e case, the two methods have the approximately $O(\sqrt{\Delta t})$ time-step accuracy computed from log of the error ratio $r = \log_2 R$. Our convergence results differ from the result described by Bobylev and Nanbu in [7]. According to their derivation of the time–explicit formula, the order of time-step error is formally $O(\Delta t)$, but our simulation studies with the number of particles and the number of collisions per particle per time step fixed found the accumulated error scales as $O(\sqrt{\Delta t})$. By reducing the number of collisions when we increased the time step, the statistical errors associated with the random number sampling increased, scaling as $O(\sqrt{\Delta t})$. This scaling is consistent with the approximate scaling observed in the simulations.

In the e–e case and e–i case, the statistical fluctuations $\sigma^2(\cdot, N)$ are independent of time step Δt when N is kept fixed.

When Δt is held constant, the fluctuations $\sigma^2(\Delta t, \cdot)$ diminish linearly when the number of particles N grows. In our analysis, the overall errors come from two sources: deterministic errors due to the time step and random errors due to the number of particles. Another similarity between the two methods is that the errors originating from one source – either time step Δt or number of particles N – may dominate the total errors. For example, to see the decrease in errors when Δt decreases, N has to be large enough and Δt cannot be too small. Once

Δt becomes too small, we cannot see any improvement in accuracy when reducing the time step Δt unless we increase the number of particles N .

While both methods have the same order of accuracy $O(\sqrt{\Delta t})$ in the e–e case (with one collision per particle per time step), Nanbu’s method is more accurate. Specifically, it produces a time-step error that is smaller by a factor of 1/2, i.e.,

$$e_{\text{DNanbu}}(\Delta t, N) \approx \frac{1}{2} e_{\text{DTA}}(\Delta t, N)$$

This means that Nanbu’s method can use $4\Delta t$ to achieve the same accurate results as TA’s method. This translates to a considerable savings in time and cost.

Nanbu’s method is more complicated and therefore harder to implement. Nanbu’s method involves solving a nonlinear function for A for every s . However, the value of A can be computed in advance and stored in a table; therefore, this disadvantage is not that significant because ultimately it does not slow down the computation.

To conclude, many similarities exist between the two methods. However, we note the advantage of Nanbu’s method in reducing the computational cost and achieving higher accuracy. We are currently exploiting Nanbu’s method in extending the earlier hybrid method developed for rarefied gas to the simulation of plasmas with Coulomb collisions with improved computational efficiency.

Acknowledgments

The work of Wang, Lin and Cafilisch was supported in part by grant DE-FG02-05ER25710 from the U.S. Department of Energy. The work of Cohen and Dimits was performed under the auspices of the U.S. Department of Energy by the Lawrence Livermore National Laboratory in part under Contract W-7405-Eng-48 and in part under Contract DE-AC52-07NA27344.

References

- [1] O.V. Batishchev, M.M. Shoucri, A.A. Batishcheva, I.P. Shkarofsky, *J. Plasma Phys.* 61 (part 2) (1999) 347.
- [2] L. Spitzer Jr., *Physics of Fully Ionized Gases*, second ed., Interscience, New York, 1967.
- [3] T. Takizuka, H. Abe, *J. Comput. Phys.* 25 (1977).
- [4] K. Nanbu, *Phys. Rev. E* 55 (1997).
- [5] R.E. Cafilisch, L. Pareschi, *J. Comput. Phys.* 154 (1999) 96.
- [6] L. Landau, *Zh. Eksp. Teor. Fiz.* 7 (1937) 203;
L. Landau, *Phys. Z. Sowjetunion* 10 (1936) 154.
- [7] A.V. Bobylev, K. Nanbu, *Phys. Rev. E* 61 (4) (2000) 4576.
- [8] M.N. Rosenbluth, W.M. MacDonald, D.L. Judd, *Phys. Rev.* 107 (1957) 1.
- [9] B.A. Trubnikov, *Review of Plasma Physics*, vol. 1, Consultant Bureau, New York, 1965, p. 105.